Very-long distance propagation of high-energy laser pulse in air

Jingwei Wang,[1,2,*] Wei Yu,[1] M. Y. Yu,[3,4,5] Sergey Rykovanov,[2,6] Jingjing Ju,[1]
Shixia Luan,[1] Kun Li,[1] Yuxin Leng,[1] Ruxin Li,[1] and Zheng-Ming Sheng[7,8]

[1] *State Key Laboratory of High Field Laser Physics, Shanghai Institute of Optics and Fine Mechanics, Chinese Academy of Sciences, Shanghai 201800, China*

[2] *Helmholtz Institute Jena, Fröbelstieg 3, 07743 Jena, Germany*

[3] *Center for Advanced Material Diagnostic Technology, Shenzhen Technology University, Shenzhen 518118, China*

[4] *Institute for Fusion Theory and Simulation, Zhejiang University, Hangzhou 310027, China*

[5] *Institute for Theoretical Physics I, Ruhr University, D-44780 Bochum, Germany*

[6] *Center for Computational and Data-Intensive Science and Engineering, Skolkovo Institute of Science and Technology, Moscow, Russia 121205*

[7] *Key Laboratory for Laser Plasmas of the Ministry of Education, School of Physics and Astronomy, Shanghai Jiao Tong University, Shanghai 200240, China*

[8] *SUPA, Department of Physics, University of Strathclyde, Glasgow G4 0NG, United Kingdom*

(Dated: October 30, 2018)

Long distance propagation of an energetic laser pulse with intensity slightly below that for multi-photon ionization (MPI) in air is considered analytically, by noting that in the process it is mainly the peak region of the pulse that interacts with the air molecules. Similar to that of much shorter femtosecond laser pulses of similar intensity, the affected air becomes slightly ionized and self-consistently forms a co-propagating thin and low-density plasma filament along the axis. It is found that a hundred-Joule-level laser pulse with relatively large spot radius and pulse duration can propagate (also in the form of a self-consistent filament) tens of kilometers through the atmosphere. Such laser propagation properties should have applications in many areas.

I. INTRODUCTION

Long-distance propagation of intense short laser pulse in air much beyond the Rayleigh length has been found since two decades ago [1–3], i.e., suitably intense short laser pulses can propagate in air for distances much longer than the Rayleigh length. This phenomenon has many practical applications, such as for atmosphere diagnostics and modification, etc. [4–15], and has been intensively studied [16–19]. This interesting process occurs as a result of marginal yet self-balanced focusing and plasma defocusing of the laser light: the intense peak region of the femtosecond laser pulse can slightly ionize (with ionization degree as low as 1%) a small amount of air molecules in its path via MPI, yet without inducing avalanche ionization and electron heating that can result in a plasma dense enough to reflect or absorb the laser light. For the main air molecules, the ionization intensity thresholds are in the range 10^{13}–$10^{15}\mathrm{W/cm^2}$, so that the peak of the focused laser should be in this regime. The ionization produced plasma tends to defocus the laser, whose intensity then again falls below the ionization threshold, so that Kerr focusing is dominated again. Since only a small fraction of laser energy is spent in the ionization, the focusing-defocusing process is repeated in a continuous manner and the laser pulse can propagate until its energy becomes too low. Moreover, as recombination of the excited air molecules takes place, the plasma along the path of the laser pulse can be readily detected as a thin filament of white light. In the process, the periphery, or the skirt, of the laser pulse is not actively involved in the interaction but acts as an energy reservoir and stabilizer for the intense light on the axis [1–3].

Unlike that in the existing works on the long distance propagation of *very short* laser pulses in air [16–19], here we consider relatively long-pulse lasers. Our analysis is based on the observation that it is mainly the peak-intensity region of the focused laser pulse that interacts with and ionizes the air molecules. More importantly, it is found that a *high-energy* laser pulse with suitable spot radius, pulse duration, and intensity can propagate tens of kilometers through the atmosphere at relatively low altitudes with significant amount of energy to spare. Such a very long distance laser propagation in air should be suitable for low-angle low-altitude detection, diagnostic, and other purposes.

II. THE MODE OF LASER PROPAGATION IN AIR

The envelope of the vector potential of a Gaussian laser pulse propagating in the z direction can be represented by [20] $a(\rho, z, \zeta) = a_0 u(\rho, z) \exp(-\zeta^2/2\tau^2)$, where $\zeta = t - z$, a_0 is the peak amplitude (normalized by mc^2/e, m is the electron mass, c is the vacuum light speed, and $-e$ is the electron charge) and $u(\rho, z)$ is the spatial profile of the pulse. We have assumed that the pulse is azimuthal

* jwwang03@gmail.com

symmetric, and normalized ρ and z by the wavelength $\lambda = 2\pi c/\omega$, and t and τ by the period $2\pi/\omega$, respectively, of the laser light in vacuum, with ω the laser frequency. We note that in air or very-low density unmagnetized plasma, the group velocity of light is effectively c. Accordingly, one can write the intensity for a Gaussian laser $I(\rho, z, \zeta) = a_0^2 I_n |u(\rho, z)|^2 \exp(-\zeta^2/\tau^2)/8\pi$, where $I_n = m^2\omega^2 c^3/e^2 \sim 3.47 \times 10^{19}$ W/cm^2 for $\lambda = 1\mu$m.

We consider a laser with pulse duration τ and timescale of variation much larger than the light wave period $2\pi/\omega$. The equation for the envelope $u(\rho, z)$ of the laser vector potential under the paraxial approximation can be written as [20]

$$2i\partial_z u(\rho, z) + \rho^{-1}\partial_\rho \left[\rho \partial_\rho u(\rho, z)\right] = (1 - \varepsilon_1)\, u(\rho, z). \quad (1)$$

As what we did in the laser propagation in plasmas [21], we assume $u(\rho, z) = v(z) \exp[-q(z)\rho^2]$, with $v(z)$ real and $q(z) = b^{-2}(z) + iR^{-2}(z)$ complex, where $b(z)$, $R(z) = z(1 + z_R^2/z^2)$ and z_R are the laser spot radius, curvature radius, and Rayleigh length, respectively. Here, ε_1 is the complex dielectric constant of air (to be discussed in the next section).

Integrating (1) over $\rho d\rho$ for ρ from 0 to ∞, one obtains for the evolution of v and q:

$$i\partial_z (v/q) = v \int_0^\infty (1 - \varepsilon_r) \exp\left(-q\rho^2\right) \rho d\rho, \quad (2)$$

and the rate of energy loss by the laser pulse during its propagation is

$$\partial_z \left(v^2 b^2\right) = -4v^2 \int_0^\infty \varepsilon_i \exp\left(-2\rho^2/b^2\right) \rho d\rho, \quad (3)$$

where the subscripts r and i denote the real and imaginary parts of ε_1, respectively.

We now consider the dielectric properties of air. Taking into account Kerr focusing and MPI, the dielectric constant ε_1 of air can be written as [8, 16–19]

$$\varepsilon_1 = 1 + \eta_2 I - n_0 + i\varepsilon_i, \quad (4)$$

where the four terms on the right correspond to contributions from linear dispersion, nonlinear Kerr focusing, MPI electron defocusing, and dissipative effects, respectively. Here, $\eta_2 \sim 5 \times 10^{-19}$ cm^2/W is the nonlinear refractivity of air, I is the laser intensity, n_0 is the normalized (say, by the critical density $n_c = m\omega^2/4\pi e^2$) density of the MPI free electrons, and ε_i the energy loss. The Kerr term can also be expressed in terms of the laser power $P = 2\pi \int_0^\infty I\rho d\rho$ as $P/P_{\rm thres}$ [20, 22], where $P_{\rm thres}$ is the threshold power for Kerr focusing. This expression is useful when the laser power and spot radius are explicitly known, such as in experimental determinations of the refractive index of a medium.

For the laser-intensity regime of interest here, the MPI electron density can be written as [20]

$$n_0(\rho, z, \zeta) = N_p^{3/2} n_{\rm air} \int_{-\infty}^{\zeta} \left[\pi I(\rho, z, \zeta')/E_i\right]^{N_p} d\zeta', \quad (5)$$

where $N_p = 11$ is the minimum number of photons required for MPI, $n_{\rm air}$ is the normalized (by n_c) density of the background air, I is the laser intensity normalized by I_n, and $E_i = 12$ eV$/mc^2 = 2.3 \times 10^{-5}$ is the normalized ionization potential. Since MPI takes place mainly near the peak ($\zeta \sim 0$) of the Kerr focused laser pulse, we have

$$\begin{aligned} n_0(\rho, z) &= N_p^{3/2} n_{\rm air} \int_{-\infty}^{0} \left[I(\rho, z, \zeta')/2I_{\rm thres}\right]^{N_p} d\zeta' \\ &= \alpha_2 \left(I_L/2I_{\rm thres}\right)^{N_p} |u(\rho, z)|^{2N_p}, \end{aligned} \quad (6)$$

where $\alpha_2 = \sqrt{\pi}\tau n_{\rm air} N_p/2$, $I_{\rm thres} = E_i/2\pi = 0.36 \times 10^{-5}$ is the threshold intensity for MPI, and $I_L = a_0^2/8\pi$. We further assume that the laser energy loss is mainly due to the MPI, i.e., $\varepsilon_i I \sim n_0 N_p E_{\rm photon}$. Accordingly, at $\zeta \sim 0$ we have

$$\varepsilon_i(\rho, z) = \frac{\alpha_2 N_p E_{\rm photon}}{2I_{\rm thres}} \left(\frac{I_L |u(\rho, z)|^2}{2I_{\rm thres}}\right)^{N_p - 1}, \quad (7)$$

where $E_{\rm photon} = \hbar\omega/mc^2$ is the normalized photon energy. Together with (6) for the MPI electron density, one can then numerically solve (2).

III. LASER SELF-GUIDING IN AIR

We are interested in self-guiding of laser that can lead to steady long-distance propagation without inducing avalanche ionization of the affected air. Accordingly, the laser spot radius should remain unchanged for as long as possible. Thus, we require

$$\partial_z b = 0, \quad (8)$$

which determines the initial parameters of the laser pulse.

In view of the recent interest in the long distance propagation of very short, or femtosecond, laser pulses in air, it is instructive to first consider a relatively short laser pulse. Figure 1 is for an incident laser pulse of duration 100 fs, wavelength $1\mu m$, spot radius $b_0 = b(z = 0) = 100\ \mu m$, peak intensity 3.5×10^{13} W/cm^2, and laser energy 1.1 mJ. The initial spot radius b_0 has been chosen to match the conditions (8). We can see in Fig. 1 that the laser spot and plasma radii diverge, and after 50 m only about 20% of the laser energy is left. As mentioned, such laser propagation much beyond the Rayleigh length is made possible by a self-regulating balance between Kerr focusing, and plasma-induced defocusing in a small region on the axis of the laser pulse. Note that this scenario is quite different from that of the guiding of ultra-intense lasers in pre- or self-formed plasma channels produced when the plasma electrons are driven out by the strong light pressure. In that case the plasma creation and laser propagation mechanisms are very different from that considered here, in particular, the laser light is inside rather than outside the plasma channel [21, 23–25].

Fig. 2 shows the radial profiles of the laser intensity and the electron density at $z = 20$ m. We see that

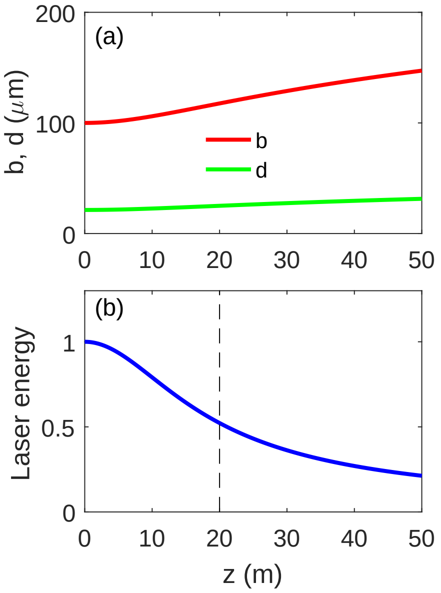

FIG. 1. Evolution of the (a) laser spot b (red curve) and electron channel radius d (green curve), (b) laser energy. The initial laser parameters are: peak normalized intensity $a_0 = 0.005$ (or 3.5×10^{13} W/cm^2), wavelength $\lambda = 1$ μm, spot radius $b_0 = 100$ μm, and pulse duration $\tau = 100$ fs, corresponding to an energy of 1.1 mJ. The pristine air density is $n_{\rm air} = 10^{19}$ cm^{-3}.

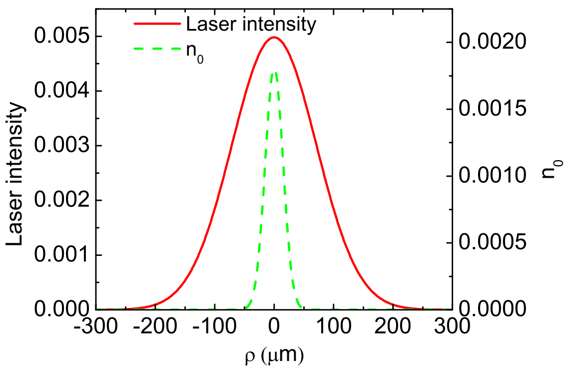

FIG. 2. Radial profiles of the normalized laser intensity and normalized (by the air density) MPI-electron density (green curve) at $z = 20$ m. The laser and air parameters are the same as in Fig. 1. Note that the free electrons are of very low density, only $\sim 0.002 n_{\rm air}$ (with the ionization degree less than 1%), and are well localized inside the laser light.

the MPI free electrons are of very low density, namely $\sim 0.002 n_{\rm air}$, and the corresponding ionization degree is less than 1%. They are also well localized in the peak region of the laser pulse. However, because of the slow but finite energy loss as it propagates, eventually the laser cannot continue to provide the Kerr focusing needed to balance the optical diffraction, so that it diverges, as can be seen in Fig. 1(a). This scenario is consistent with that investigated in the experiments and theories of short-

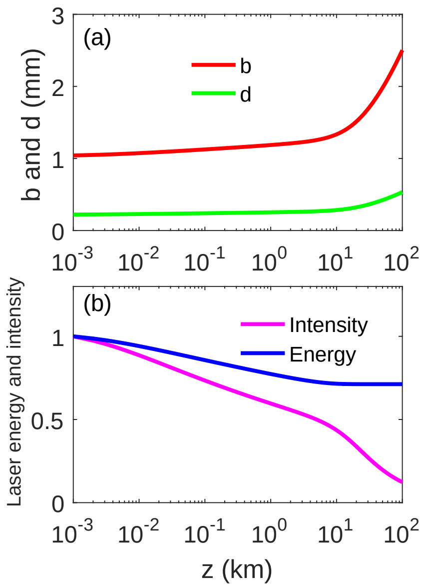

FIG. 3. (a) Evolution of the laser spot radius b (red curve) and plasma radius d (green curve), and (b) the normalized (by $E_0 = E(0)$) laser energy E (blue curve) and the normalized (by $I_0 = I(0)$) spot-size dependent intensity I (magenta curve), for a 33 ps laser pulse with initial spot radius $b_0 = 1$ mm, corresponding to an energy of 36 J. The other parameters are the same as that in Fig. 1. Note that the horizontal axes are in units of kilometers.

pulse laser propagation in air [1–3, 16–19].

IV. LONG DISTANCE LASER PROPAGATION IN AIR

The preceding result indicates that the propagation distance of the laser is limited by light energy loss. One can thus expect prolonged propagation distance by employing a longer-pulse larger-spot laser, i.e., a laser of high initial energy but with intensity just below that for MPI to occur. Fig. 3 is for a laser with pulse duration $\tau = 33$ ps, spot size $b_0 = 1$ mm and energy 36 J. We see that such a tens-picosecond laser pulse can propagate in a self-guided manner for tens of kilometers with its intensity still around 10^{12} W/cm^2. One can calculate that, after a distance of 10 km, the energy consumed by MPI is about 12 J. That means more than 60% laser energy still remains, which is consistent with Fig. 3(b). Long-distance laser focusing can also be achieved by elaborate focusing techniques or group-velocity-dispersion control [3], but in that case the light energy content rapidly becomes small, thereby limiting their range of applications.

For given air environment, a key controllable parameter for long-distance propagation of the laser filament is the initial laser power. Since the laser intensity is limited to near the MPI threshold in air, the relevant parameters

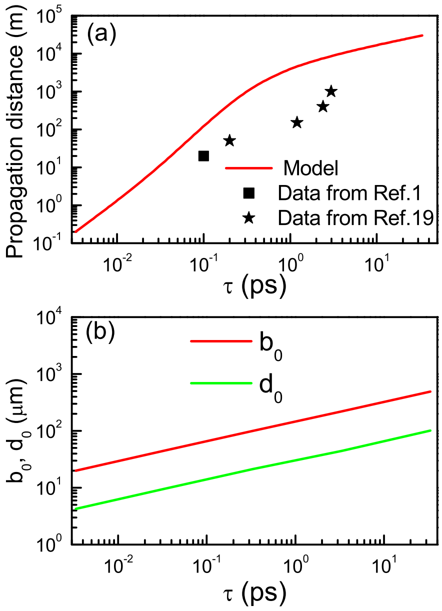

FIG. 4. (a) Effects of the laser pulse duration τ on laser propagation distance as determined by laser intensity falling to below $1/e$ of the initial value, as compared with the experimental data from Ref. [1] (square symbol) and Ref. [19] (star symbol). (b) The optimal initial laser spot b_0 (red curve) and the plasma cross section d_0 (green curve) for different τ values in the relatively steady-size regimes.

are therefore the initial pulse duration τ and initial spot radius b_0 of the laser. Fig. 4(a) shows the effect of the pulse duration τ on the laser propagation distance (defined as that at which the laser intensity becomes $1/e$ of its initial value). We see that the propagation distance starts with a near-power-law scaling with the pulse duration, but tends to saturate after $\tau \sim 0.5$ ps. Still larger τ will not be beneficial since electron heating by the too-long laser can lead to optical breakdown, so that the trailing part of the laser will be reflected and/or absorbed by the resulting plasma. The experimental data from Ref. [1] and [19] are also presented in Fig. 4(a) as a comparison. With the same duration of laser pulse, the propagation distance in our model is obviously larger than that from the experiments. The reason is probably that the nonlinear effects, such as ionization instabilities and inverse Bremsstrahlung, which will cause additional loss of laser energy, are not included in the model. We notice that Fig. 4(b) shows the dependence of the optimal initial laser spot b_0 and plasma radius d_0 on τ in the relatively steady regimes of laser propagation. From the log-log plot, we see that they have the same power-law scaling, indicating that the plasma profile follows closely that of the paraxial laser pulse, as to be expected for steady propagation.

V. LASER PROPAGATION WITH QUASI-PERIODIC FOCUSING AND DEFOCUSING

In the above we have considered relatively steady propagation of the laser pulse, where Kerr focusing and MPI-electron defocusing balance each other, by carefully choosing the input laser parameters. However, other evolution scenarios of the laser-air interaction are also possible. Accordingly, we next consider non-steady laser propagation.

It may be instructive to briefly review the initial stage of the long-distance self-focusing process, which determines the type of laser propagation. If the laser intensity is too low, it would be difficult to start the initial MPI, and therefore the laser self-guiding will not happen. However, if the total laser power is initially larger than the threshold power for Kerr focusing, the laser spot radius will gradually decrease, together with increase of the peak laser intensity until the peak intensity exceeds the MPI threshold of air. When MPI happens, a mass of MPI free electrons will be created. The plasma defocusing then becomes dominated and the intensity of the incident laser quickly decreases. If the remaining laser power, after the MPI process, is lower than the threshold for Kerr focusing, the laser pulse will fully defocus. On the other hand, if the laser power remains higher than the threshold for Kerr effect, the defocused light will be focused again. Since only little energy (compared with that in the laser pulse) is spent in each MPI event. The focusing-defocusing process is repeated until the laser power becomes too low. For example, Fig. 5 shows multi-focusing of a laser pulse with initial intensity $I_0 = 5.0 \times 10^{12}$ W/cm^2, pulse duration 1 ps, and initial spot radius 5 mm. One can see that the focusing-defocusing process is repeated with decreasing peak amplitude, appearing as a quasi-periodic series of roughly half-meter-long pulses of EM radiation. In this case, the intensity decays more rapidly, since more energy is spent in the focusing-defocusing process. They have also been observed in the experiments [26].

VI. CONCLUSION

In contrast to guidance of laser pulses by preformed or interaction-generated plasma channels involving high-intensity lasers and high-density plasmas [21, 25, 27], here the MPI-generated plasma is of much lower density and its cross section is much less than that of the laser light. It should be emphasized that here the laser intensity must be such that it remains very close to the MPI threshold, so that the resulting MPI free electrons are of low energy and density. Otherwise optical-breakdown (avalanche ionization), and effects such as ionization instabilities, inverse Bremsstrahlung, plasma expansion, etc., which can lead to defocusing and absorption of the laser light, would have to be taken into consideration [4, 7, 20].

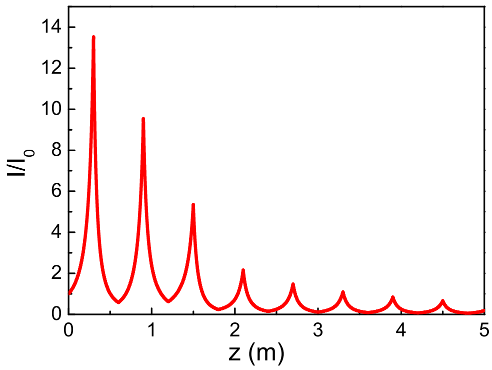

FIG. 5. Normalized intensity I/I_0 for periodic focusing and defocusing of laser light. Here the initial laser intensity is $I_0 = 5.0 \times 10^{12}$ W/cm^2, the spot radius and duration are 5 mm and 1 ps, respectively. The other parameters are the same as in Fig. 1.

We have also assumed that the background air is of uniform density and quiescent. In applications such as long-distance diagnostics of the atmosphere, one would have to modify the dielectric constant ε_1 by taking into account nonuniform air density and possible encounters with clouds, dusts, etc [14, 15, 17, 19]. However, the laser pulse should not be slowed down, otherwise avalanche ionization can easily occur. Moreover, our analysis is not applicable at too-high altitudes, where the background air can contain plasma photo-ionized by sunlight.

In conclusion, we have considered a relatively simple model for long-distance laser propagation in air. The model is based on the fact that it is mainly the intense peak of the focused laser pulse that directly interacts with the air molecules, so that one needs only to consider the MPI process on the laser axis. It is shown that a large-spot long-pulse laser of high energy but near-MPI-threshold intensity can travel tens of kilometers through the atmosphere at high-energy level. The results should be useful for long-distance diagnostics of the atmosphere, long-distance excitation and guidance of natural or artificial lightning discharge or charged-particle beams, remote deposition of laser energy, etc. Our approach can also be applied to other laser driven processes [4, 28–31], where the peak intensity of the laser pulse plays an important role.

ACKNOWLEDGMENTS

This work was supported by the National Natural Science Foundation of China (11674341, 11675245, 11374262, 11775144), the National Basic Research Program of China (2013CBA01504) and Strategic Priority Research Program (B) of Chinese Academy of Sciences (No. XDB160104). MYY also acknowledges support from the State Key Laboratory of High Field Laser Physics at SIOM.

[1] A. Braun, G. Korn, X. Liu, D. Du, J. Squier, and G. Mourou, Opt. Lett. **20**, 73 (1995).
[2] L. Wöste, C. Wedekind, H. Wille, P. Rairoux, B. Stein, S. Nikolov, C. Werner, S. Niedermeier, F. Ronneberger, H. Schillinger, R. Sauerbrey, Laser Optoelektron. **29**, 51 (1997).
[3] P. Rairoux, H. Schillinger, S. Niedermeier, M. Rodriguez, F. Ronneberger, R. Sauerbrey, B. Stein, D. Waite, C. Wedekind, H. Wille, L. Wöste, and C. Ziener, Appl. Phys. B **71**, 573 (2000).
[4] A. Sergeev, E. Vanin, L. Stenflo, D. Anderson, M. Lisak, M. L. Quiroga-Teixeiro, Phys. Rev. A **46**, 7830 (1992).
[5] A. K. Dharmadhikari, J. A. Dharmadhikari, and D. Mathur, Appl. Phys. B **94**, 259 (2009).
[6] H. Wille, M. Rodriguez, J. Kasparian, D. Mondelain, J. Yu, A. Mysyrowicz, R. Sauerbrey, J. P. Wolf, L. Wöste, Eur. Phys. J. Appl. Phys. **20**, 183 (2002).
[7] J. Kasparian, M. Rodriguez, G. Mèjean, J. Yu, E. Salmon, H. Wille, R. Bourayou, S. Frey, Y,-B. André, A. Mysyrowicz, R. Sauerbrey, J.-P. Wolf, and L. Wöste, Science **301**, 61 (2003).
[8] W. Yu, M. Y. Yu, J. Zhang, L.J. Qian, X. Yuan, P. X. Lu, R. X. Li, Z. M. Sheng, J. R. Liu, Z. Z. Xu, Phys. Plasmas **11**, 5360 (2004).
[9] L. Wöste, S. Frey, J.-P. Wolf, Adv. Atom., Mol. Opt. Phys. **53**, 413 (2006),
[10] H. Yang, J. Zhang, Y. J. Li, J. Zhang, Y. T. Li, Z. L. Chen, H. Teng, Z. Y. Wei, and Z. M. Sheng, Phys. Rev. E **66**, 016406 (2002).
[11] P. Rohwetter, J. Kasparian, K. Stelmaszczyk, Z. Hao, S. Henin, N. Lascoux, W. M. Nakaema, Y. Petit, M. Queisser, R. Salamé, E. Salmon, L. Wöste, and J.-P. Wolf, Nat. Photon. **4**, 451 (2010).
[12] J. Ju, J. Liu, C. Wang, H. Sun, W. Wang, X. Ge, C. Li, S. L. Chin, R. X. Li, Z. Z. Xu, Opt. Lett. **37**, 1214 (2012).
[13] P. Polynkin and M. Kolesik, Phys. Rev. A **87** 053829 (2013).
[14] E. S. Manuilovicha, V. A. Astapenkoa, and P. A. Golovinskii, Atm. Oceanic Opt. **28**, 209 (2015).
[15] R. M. Measures, *Laser Remote Sensing: Fundamentals and Applications.* (Krieger, Malabar, Florida, 1992).
[16] P. Sprangle, J. R. Penano, and B. Hafizi, Phys. Rev. E **66**, 046418 (2002).
[17] A. Couairon and A. Mysyrowicz, Phys. Rep. **441**, 47 (2007).
[18] L. Bergé, S. Skupin, R. Nuter, J. Kasparian, J.-P. Wolf, Rep. Prog. Phys. **70**, 1633 (2007).
[19] M. Durand, A. Houard, B. Prade, A. Mysyrowicz, A. Durecu, B. Moreau, D. Fleury, O. Vasseur, H. Borchert, K. Diener, R. Schmitt, F. Theberge, M. Chateauneuf, J.-F. Daigle, and J. Dubois, Opt. Express **21**, 26836 (2013). and references therein.

[20] Y. R. Shen, *The Principles of Nonlinear Optic*s (Wiley, New York, 1984).
[21] J. W. Wang, W. Yu, M. Y. Yu, A. L. Lei, X. Wang, V. K. Senecha, X. G. Wang, M. Murakami, and K. Mima, Phys. Plasmas **17**, 103109 (2010).
[22] J. H. Marburger, Prog. Quantum Electron. **4**, 35 (1975).
[23] D. Umstadter, Phys. Plasmas **8**, 1774 (2001).
[24] B. Hafizi, A. Ting, R. F. Hubbard, P. Sprangle, and J. R. Peñano, Phys. Plasmas **10**, 1483 (2003).
[25] L. Cao, W. Yu, M. Y. Yu, X. Wang, Y. Gu, and X. T. He, Phys. Plasmas **16**, 093109 (2009).
[26] Z.-Q. Hao, J. Zhang, X. Lu, T.-T. Xi, Y.-T. Li, X.-H. Yuan, Z.-Y. Zheng, Z.-H. Wang, W.-J. Ling, and Z.-Y. Wei, Opt. Express **14**, 773 (2006).
[27] G. Kalintchenko, P. Rousseau, V. Yanovsky, A. Zigler, A. Maksimchuk, and K. Krushelnick, Phys. Plasmas **16**, 113105 (2009).
[28] V. E. Zuev, High Power Laser Radiation in Atmosphere (Consultants Bereau, New York, 1982).
[29] G. Field and D. Spergel, Science **231**, 1387 (1986).
[30] G. Méchain, A. Couairon, Y.-B. André, C. D'Amico, M. Franco, B. Prade, S. Tzortzakis, A. Mysyrowicz, and R. Sauerbrey, Appl. Phys. B **79**, 379 (2004).
[31] P. Béjot, J. Kasparian, S. Henin, V. Loriot, T. Vieillard, E. Hertz, O. Faucher, B. Lavorel, and J.-P. Wolf, Phys. Rev. Lett. **104**, 103903 (2010).